UNIVERSITY OF CALIFORNIA SAN DIEGO

Dissection of BTLA Interactomes Using Cell Free Reconstitution

A Thesis submitted in partial satisfaction of the requirements for the degree
Master of Science

in

Biology

by

Zijun Wu

Committee in charge:

Professor Enfu Hui, Chair
Professor Maho Niwa Rosen, Co-Chair
Professor Douglass Forbes

2018

The Thesis of Zijun Wu is approved and it is acceptable in quality and form for publication electronically:

Co-Chair

Chair

University of California San Diego

2018

TABLE OF CONTENTS

LIST OF ABBREVIATIONS

APC	Antigen presenting cell
BTLA	B and T lymphocyte attenuator
Co-IP	Co-immunoprecipitation
DC	Dendritic cell
FRET	Fluorescence resonance energy transfer
Grb-2	Growth factor receptor-bound protein 2
hBTLAcyto	human B and T lymphocyte attenuator cytoplasmic domain
ITIM	Tyrosine-based inhibitory motif
ITSM	Tyrosine-based switch motif
Lck	Lymphocyte-specific protein tyrosine kinase
PD-1	Programmed cell death protein 1
PI3K	Phosphatidylinositol-4,5-bisphosphate 3-kinase
PKB	protein kinase B
PKC	protein kinase C
pMHC	Peptide-loaded major histocompatibility complex
Shp1	Src homology domain 2-containing tyrosine phosphatase 1
Shp2	Src homology domain 2-containing tyrosine phosphatase 2
ZAP70	Zeta-chain-associated protein kinase 70

LIST OF FIGURES

ACKNOWLEDGEMENTS

First, I would like to thank Dr. Enfu Hui for being my advisor. Without him, I would not continue working as a research scientist in academia.

I would also like to thank Dr. Xiaozheng Xu for technical support and pointing out fallacies of my thesis.

Next, I would like to thank Dr. Maho Niwa Rosen and Dr. Douglass Forbes for serving on my committee.

Last but not least, I would like to thank my parents for providing continuous support.

ABSTRACT OF THE THESIS

Dissection of BTLA Interactomes Using Cell Free Reconstitution

by

Zijun Wu

Master of Science in Biology

University of California San Diego, 2018

Professor Enfu Hui, Chair
Professor Maho Niwa Rosen, Co-Chair

B and T lymphocyte attenuator (BTLA) is a co-inhibitory receptor expressed on T cells and B cells that is structurally and functionally related to programmed death protein-1 (PD-1), a well-established cancer immunotherapy target. Binding of T cell specific BTLA with its ligand

HVEM on antigen-presenting cells triggers tyrosine phosphorylation of the intracellular tail of BTLA, and ultimately leads to suppression of the T cell response. There is growing interest in targeting BTLA for cancer immunotherapy, yet very little is known about its biochemical mechanism and potential crosstalk with PD-1. Using a well-defined liposome reconstitution system with purified recombinant proteins, we quantitatively compared the biochemical specificities of BTLA and PD-1 and dissected the roles of each tyrosine residues within BTLA using purified BTLA proteins containing point mutants. These experiments reveal unexpected differences in BTLA and PD-1 specificities, which might underlie their functional disparities.

INTRODUCTION

T cell activation

T lymphocytes play essential roles in adaptive immunity. Upon recognition of tumor cells, virus-infected cells, or professional antigen presenting cells (APCs), T cells then mount an immune response to destroy the target cell (Samelson, 1986). The activation of naïve T lymphocyte requires two types of signals: (1) the antigen-specific signal through T cell antigen-specific receptor (TCR), triggered by peptide bound to the major histocompatibility complex (pMHC) on the APC, and (2) the antigen none-specific signals mediated by co-stimulatory molecules (Pardoll, 2012). On the other hand, T cell response is negatively regulated by co-inhibitory receptors, which attenuate T cell activation upon the binding to their ligands on the target cell. The balance among the T cell receptor (TCR), co-stimulatory signals, and co-inhibitory signals determines the fate of T cells and the target cells.

TCR signaling

Many cellular processes require regulation of protein phosphorylation in signal transduction. In T cells, tyrosine phosphorylation serves to modulate the activities of enzymes and the affinities of protein-protein interactions, thereby mediating propagation of the signal. Upon TCR engagement with the peptide-loaded MHC (pMHC), the LymphoCyte-specific protein tyrosine Kinase (Lck) phosphorylates the CD3 chains of the TCR complex, causing recruitment of another kinase ZAP70 to the membrane, whereupon ZAP70 phosphorylates many downstream targets to activate the T cell (Yokosuka, 2005). Lck also acts to phosphorylate tyrosine residues within other receptors in T cells, as detailed below.

Co-stimulatory signaling

TCR signaling in the absence of co-stimulatory signals is insufficient to activate naïve T cell (Chen and Flies, 2003). Co-stimulatory receptors, such as CD28, provide the necessary positive signal to promote cell cycle progression, cytokine production, and T cell survival (Song, 2004). Upon binding to its ligand B7 on the APC, CD28 becomes tyrosine phosphorylated at the cytoplasmic tail, which then recruits phosphatidylinositol 3-kinase (PI3K) and protein kinase C (PKC). PI3K mediates phosphorylation of protein kinase B (PKB) and PKC, which in turn causes activation of nuclear distal molecules including mTOR and NFKB (Rudd, 2003).

Co-inhibitory signaling

Co-inhibitory receptors act as molecular brakes to restrain uncontrolled T cell activity and to prevent immune related tissue damage (Wang, 2005). Normally, co-inhibitory receptors are transiently expressed on T cells and decline upon the removal of TCR signal. However, persistent antigen stimulation in tumors or chronic viral infection leads to constitutive overexpression of co-inhibitory receptors, such as programmed cell death protein 1 (PD-1), B and T lymphocyte attenuator (BTLA), and V-domain Ig suppressor of T cell activation (VISTA), rendering T cells hypofunctional or exhausted (Wherry and Kurachi, 2015). In addition, the ligands for the co-inhibitory receptors are often upregulated on tumor cells or tumor infiltrating APCs. Overexpression of these inhibitory molecules is a key mechanism for a tumor to escape from immune destruction (Deppong, 2006). Monoclonal antibodies against PD-1 or CTLA-4 have demonstrated exciting clinical activities against some human cancers (Parry, 2005). Antibodies against other co-inhibitory molecules are under evaluation in clinical trials or animal models (Zhao, 2016).

PD-1

Programmed cell death protein-1 (PD-1) inhibits T cell activity upon interaction with its ligand PD-L1 (Latchman, 2011). PD-1 and PD-L1 are the most successfully clinically targeted immune checkpoint. However, the molecular mechanism by which PD-L1/PD-1 inhibit T cell response is still incompletely understood. The intracellular domain of PD-1 contains one immunoreceptor tyrosine-based inhibitory motif (ITIM) and one immunoreceptor tyrosine-based switch motif (ITSM). Upon PD-L1 binding, both the ITIM and ITSM of PD-1 become phosphorylated by the Src family kinase Lck. Phosphorylated PD-1 then recruits Src homology domain 2-containing tyrosine phosphatase 2 (Shp2), which dephosphorylates the TCR and CD28 signaling components (Hui, 2017).

BTLA

BTLA is an inhibitory cell surface receptor belonging to the CD28/B7 superfamily (Watanebe, 2003). BTLA exhibits a broad distribution on different cell types, showing high expression by B and T lymphocytes, and relatively low expression on splenic macrophages, matured bone marrow-derived dendritic cells (DCs), and natural killer cells (Han, 2004; Otsuki, 2006). Binding of BTLA by HVEM triggers suppression of T cell activation and T cell-target cell communication (Sedy, 2015). Mounting evidence suggests that BTLA can also be co-opted by viruses and tumors for immune evasion. By causing overexpression of BTLA and other inhibitory molecules on T cells, tumors are able to induce the T cells into an exhausted, dysfunctional state (del Rio, 2010).

Previously, BTLA was considered to share similar functional properties with PD-1 due to structural similarities (Chen and Flies, 2013). Like PD-1, the cytoplasmic domain of BTLA contains ITSM and ITIM (Watanabe, 2003). In addition, BTLA contains an additional potential growth factor receptor-bound protein 2 (Grb-2) interaction site (Watanabe, 2003) (Fig. 1E). Co-immunoprecipition assays have suggested that BTLA are capable of recruiting Shp1 and Shp2 (Gavrieli, 2003), Grb2 and PI3K (Gavrieli, 2006). Yet, it is unclear whether these interactions are physiological and whether these interactions are direct.

In this thesis, we clarified the BTLA interactome by using a reconstituted membrane system. In this system, purified BTLA cytoplasmic domain was reconstituted on fluorescence-labeled liposomes, and the recruitment of SH2 proteins was measured in real time by a fluorescence resonance energy transfer (FRET) approach. We also dissected the contribution of each of the four tyrosine residues within the cytoplasmic tail of BTLA in recruiting cytoplasmic effectors by carefully comparing the tyrosine mutants of BTLA with the wild-type protein.

Liposome reconstitution system

A conventional method for studying protein-protein interaction is co-immunoprecipitation, but this assay lacks kinetic information and does not prove direct interaction. In this study, we used a cell-free reconstituted system consisting of a well-defined set of components to mimic reactions occurring on membranes of T cells. In particular, we reconstituted purified BTLA or PD-1 cytoplasmic tail into liposomes that mimic the plasma membrane of T cells. In this system, tyrosine phosphorylation of BTLA or PD-1 attached on liposome membrane surface leads to translocation of SH2 proteins from the solution to the liposome membrane. We employed a FRET approach to monitor this translocation process in

real time (Hui, 2014). Compared to cell-based assays, this membrane reconstitution system provides a well-defined membrane environment that allows for measurement of specific interactions, and quantitative controls of each key component.

Fluorescence Resonance Energy Transfer (FRET)

Fluorescence resonance energy transfer (FRET) is a method to measure distances between molecules. Energy transfer only occurs when the two fluorophores (donor and acceptor) are in physical proximity (10 – 100 Å) (Wu, 1994). Binding of the two molecules would decrease their inter-molecular distance, which can be measured by FRET. In this thesis, in order to determine the translocation of protein to membranes, we labeled the protein of interest with a donor fluorophore using a genetically fused SNAP tag, and the membrane with an acceptor fluorophore using Rhodmine-PE lipid. Immediately after receptor phosphorylation, time-resolved distance reduction between the protein of interest and the liposome lead to FRET, as reflected by a decrease in the donor fluorescence (Hui, 2014).

MATERIALS AND METHODS

Reagents

Synthetic 1,2-dioleyl-sn-glycero-3-phosphocholine (POPC), 1-palmitoyl-2-oleoyl-*sn*-glycero-3- phospho-L-serine (POPS), 1,2-dioleoyl-sn-glycero-3-[(N-(5-amino-1-carboxypentyl)iminodiacetic acid)succinyl] (nickel salt, DGS-NTA-Ni), N-(lissamine rhodamine B sulfonyl)-1,2-dipalmitoyl-sn-glycero-3 phosphoethanolamine (Rhodamine-PE), and 1,2-dioleoyl-sn-glycero-3-phosphoethanolamine-N-[methoxy(polyethylene glycol)-5000] (ammonium salt) (PEG5000 PE) were purchased from Avanti Polar Lipids.

Plasmid Construction

The full-length human BTLA gene block was purchased from GE (Catalog # MHS6278-211689762). The coding sequence of human BTLA cytoplasmic domain (hBTLAcyto) (aa196-adding TwinSTREP tag) was amplified using Phusion polymerase with the following primers:

(1) Forward: tggacagcaaatgggtcgcggaGACACAGCAGGAAGGGAAA

(2) Reverse: TCCACCTTTCTCGAACTGCGGGTGGCTCCAGGATCCactcctcacacatatgg

(3) Forward':

AGTTCGAGAAAGGTGGAGGTTCCGGAGGTGGATCGGGAGGTGGATCGTGGAGC

(4) Reverse':

gcttgtcgacggagctcgaaTTATTTTTCGAACTGCGGGTGGCTCCACGATCCACCTC

hBTLAcyto was amplified using forward (1) and reverse (2) primers first. To generate the Twinstrep tag coding sequence, forward' (3) and reverse' (4) primers were annealed together, and the complete double strand DNA segment was then produced by the DNA polymerase.

Afterward, the hBTLAcyto coding fragment and the TwinStrep tag fragment and was annealed for 6 cycles, after which a 30 cycles amplification reaction was run in the presence of the forward (1) and reverse' (4). The PCR product was sub-cloned into pET28a vector by Phusion High Fidelity, resulting in the extracellular domain of BTLA replaced by a decahistidine (His_{10}) tag at N-terminus (His_{10}-hBTLAcyto). Constructs were all verified by sequencing and alignment to the construct map.

Construction of Tyrosine to Phenylalanine BTLA Variants

Single tyrosine to phenylalanine mutations of hBTLAcyto were produced using Quick Change mutagenesis. For this, pairs of oligonucleotides were as follow:

(1) Y226F forward: GCTATCAGAAACTGGAATTTtTGATAATGACCCTGACCTTT
(2) Y226F reverse: AAAGGTCAGGGTCATTATCAaAAATTCCAGTTTCTGATAGC
(3) Y243F forward: GCAGGAAGGGTCTGAAGTTTtTTCTAATCCATGCCTGGAAG
(4) Y243F reverse: CTTCCAGGCATGGATTAGAAaAAACTTCAGACCCTTCCTGC
(5) Y257F forward: AAACAAACCAGGCATTGTTTtTGCTTCCCTGAACCATTCTG
(6) Y257F reverse: CAGAATGGTTCAGGGAAGCAaAAACAATGCCTGGTTTGTTT
(7) Y282F forward: GTAAAAGAAGCACCAACAGAATtTGCATCCATATGTGTGAGG
(8) Y282F reverse: CCTCACACATATGGATGCAaATTCTGTTGGTGCTTCTTTTAC.

Each mutant was verified by sequencing and alignment.

Recombinant Protein Expression and Purification

Transformed BL21(DE3) was grown in sterilized auto-induction medium (1% Tryptone, 0.5% yeast extract, 0.5% glycerol, 0.2% lactose, 0.05% glucose, 2 mM $MgSO_2$, 6 mM KH_2PO_4,

0.3 M K_2HPO_4, 25 mM $(NH_4)_2SO_4$) with 150 µg/mL kanamycin in a 20˚C/250 rpm shaker, until the optical density in 600 nm reached 0.6 for full induction. The volume of the bacterial culture was kept below 10% volume of the flask container, allowing sufficient inner air exchange. After more than 20 hours of incubation at 20˚C, the bacterial cells were spun down at 4000 rpm for 10 min, and then resuspended in 20 mL of cold lysis buffer [20mM HEPES-NaOH (pH 7.5), 150 mM NaCl, 20mM bME, 5% Glycerol, 1% triton, 1mM PMSF]. All following procedures were conducted at 4˚C. Whole cell lysate was obtained by sonication with an output frequency of 20 kHz, and 50% duty cycle for 5 minutes, and rested for another 5 minutes to cool down the lysate. This cycle was repeated 3 times for each protein. A cleared cell lysate was obtained by high-speed centrifugation at 30,000 xg, 4 ºC for 15 min. We used an ÄKTA chromatography system (GE Healthcare) for purification steps. StrepTrap HP column (GE Healthcare 28907547) was used to separate TwinStrep-tagged proteins and the Strep-tagged proteins were eluted with elution buffer [20 mM HEPES-NaOH (pH 7.5), 150 mM NaCl, 20 mM bME, 5% Glycerol, 1 mM desthiobiotin]. To determine the fraction containing the desired recombinant proteins, proteins were sampled and then examined by SDS-PAGE. Collected proteins were next subjected to gel filtration chromatography by Superdex 200 Increase 10/300 GL (GE Healthcare 28-9909-44) in gel filtration buffer (20 mM HEPES-NaOH (pH 7.5), 150 mM NaCl, 10% Glycerol, 2 mM TCEP). Monomer fractions were collected according to column volume, and were verified by SDS-PAGE and Coomassie staining. The resulting wild type and mutant recombinant proteins were snap frozen in liquid nitrogen and stored in -80˚C.

Protein Quantification

Purified wild type hBTLAcyto, mutant hBTLAcyto, and PD-1cyto were run with BSA standards on 13% SDS polyacrylamide gels. Gel images were captured by an Epson scanner and analyzed by ImageJ. Concentrations of the proteins were calculated from a BSA standard curve.

Preparation of Liposomes

Phospholipids consisting of 0.3% Rhod-PE + 10% DGS-NTA(Ni) + 10% DOPS + 79.7% POPC were combined. The lipid mixture was dried under N_2 gas while heated in a 50˚C water bath. To further remove moisture, the lipids were desiccated for 3 hours in the dark. The dried phospholipids were resuspended in 1x kinase buffer [50 mM HEPES-NaOH (pH 7.5), 150 mM NaCl, 10mM $MgCl_2$, 1mM TCEP]. Mini Extruder (Avanti Polar Lipid 610000) was assembled with two pieces of 200nm polycarbonate membranes stacked together in the middle, following manufacturer's instructions. The liposome suspension was extruded through the membranes at least 20 times, during which the lipid aggregates are converted to a homogeneous lipid solution.

Reconstitution Assay of Membrane-Bound Recombinant Proteins

FRET assays were carried out at room temperature in solid white, 96-well polystyrene plates (Corning 3362) in a total volume of 70 µL per reaction. For this, 0.3 mM receptor proteins, 0.3 mg/ml BSA, 1 µM His_{10}-Lck and each SH2-containing protein at 0.1 mM were premixed with 5% liposomes. The system was incubated at room temperature for 20-40 minute to enable membrane attachment till reaching a steady state. SNAP505 fluorescence traces were monitored at minimum interval (1.5 seconds). Subsequently, 1 mM ATP in 1x kinase buffer [50 mM HEPES-NaOH (pH 7.5), 150 mM NaCl, 10mM $MgCl_2$, 1mM TCEP] was added and rapidly mixed. The dynamics of SNAP505 fluorescence were further monitored. Data were normalized

by the average of the last 10 data points before ATP addition, set as 100% fluorescence. The time point of ATP addition was set as 0 min.

RESULTS

BTLA directly binds to a variety of SH2 proteins

Previous studies reported co-immunoprecipitation of BTLA with protein tyrosine phosphatases, including the protein tyrosine phosphatases Shp1 and Shp2, the lipid phosphatase SHIP-1, the kinase ZAP70, as well as adaptor proteins Grb2 and PI3K (Watanabe, 2003; Gavrieli 2003; Gavrieli, 2006). However, it is not known whether the interactions observed are direct or indirect, and the relative strength of the interactions is difficult to deduce due to the different expression levels of the SH2 proteins. In this thesis, we quantitated the ability of BTLA to recruit the aforementioned SH2 proteins using a well-defined membrane reconstitution system and a FRET readout (Fig. 3, Fig. 4, Fig.5). To this end, we attached the cytoplasmic tail of BTLA to a liposome which mimics the plasma membrane of T cells. To monitor the BTLA-dependent recruitment of SH2 proteins with FRET, we labeled the SH2 protein of interest with SNAP-cell-505 (energy donor), and Rhodamine-PE incorporated into the liposome as the energy acceptor, as described previously (Hui, 2014). This membrane reconstitution FRET assay enabled us to monitor the direct and dynamic interactions between BTLA and SH2 containing proteins. Using the reconstitution assay, we observed the recruitment of tandem SH2 domains of Shp1 ($Shp1^{tSH2}$), Shp2 ($Shp2^{tSH2}$), and PI3K (p50α) by BTLA and by PD-1 (Fig. 3). This argues for their direct binding to the checkpoint inhibitors BTLA and PD-1. However, we were not able to detect the association of Grb-2 or SHIP-1 at equivalent concentration. This suggests that the BTLA binding to these proteins is either weak or indirect. Strikingly, we found that ZAP70, a protein well known as the

major effector of the TCR, also bound to the cytoplasmic tail of BTLA. The physiological significance of this interaction warrant further investigation.

BTLA and PD-1 exhibit different binding preferences of SH2 proteins

BTLA and PD-1 are inhibitory T cell surface receptors and both belong to the B7/CD28 superfamily. Moreover, their cytoplasmic tails appear to contain similar tyrosine motifs. Therefore, we next asked whether these two checkpoint receptors recruit a similar set of SH2 proteins. We detected multiple interesting differences in their preferences using the quantitative reconstituted FRET assay. First, we confirmed that PD-1 preferentially recruits Shp2 over Shp1 (Fig. 3B), as reflected by the different speed of SNAP505 fluorescence decrease. This result is in agreement with previous work in which more Shp2 is detected in PD-1 immunoprecipiates (Parry, 2005; Yokosuka, 2012). In contrast, BTLA exhibits the same degree of Shp1 and Shp2 binding (Fig. 3A), suggesting that Shp1 might play a more important role in BTLA signaling than in PD-1 signaling. In addition, we also observed association of the subunit of PI3K, p50α, for both PD-1 and BTLA, but BTLA has substantially greater PI3K binding affinity than PD-1 (Fig. 3C). Finally, the BTLA cytoplasmic domain interacts with ZAP70 as described, whereas no ZAP70 recruitment was detected when BTLA was replaced with PD-1 (Fig. 3).

Point mutations reveal the major binding sites of Shp1, Shp2, ZAP70, and PI3K in BTLA

Having screened the possible effector molecules that can associate with phosphorylated BTLA, we next dissected the contribution of each tyrosine motif in the

recruitment of each SH2 protein. To this end, we replaced each of the four tyrosines (Y) in the cytoplasmic tail of BTLA with phenylalanine (F) via site-directed mutagenesis (Fig. 4F) and asked how each point mutation affects the recruitment of the BTLA binding proteins (Fig. 4A-E). Side by side comparisons of the four variants of BTLA revealed that no single point mutation can completely abrogate BTLA cytoplasmic functions, which is consistent with previous reports (Watanabe, 2003; Gavrieli 2006; Gavrieli, 2006). However, we detected clear preference of the tyrosine motifs to certain SH2 proteins. Mutation of the first tyrosine, i.e., the previously reported Grb-2 binding site (Y226F) specifically disrupted PI3K (p50α) binding (Fig. 4E), with no detectable effect on the recruitment of other SH2 proteins (Fig. 4B-D). Mutation of the second tyrosine (Y243F) decreased the recruitment of the tandem SH2 domains of both ZAP70 ($ZAP70^{tSH2}$) (Fig. 4D) and PI3K (p50α) (Fig. 4E). Although Y243 of the BTLA cytoplasmic tail is not conserved between human and mouse, this tyrosine clearly contributes to tyrosine kinase recruitment, as its mutation causes suppression of both ZAP70 and PI3K association. This tyrosine raises questions as to possible mechanism variances in different species. Mutation of the third tyrosine within the ITIM (Y257F) led to the strongest defect in recruitment of Shp1, Shp2 and ZAP70, and a mild defect in PI3K. These data suggest that the ITIM motif is the major binding sites for both tyrosine kinases and tyrosine phosphatases, but not lipid kinases. Mutation of the fourth tyrosine (Y282F) produced somewhat confusing results, as this mutations seemed to increase the extent of Shp1 (Fig. 4B) and Shp2 (Fig. 4C) recruitment, though with a much slower kinetics. The molecular basis of this result remain unclear, but may suggest some synergy or competition between different tyrosine motifs (Fig. 4, Fig. 6).

PD-1 mutants uncover the specificity of Shp1, Shp2, and PI3K recruitment

After dissecting the roles of individual tyrosine motifs within the BTLA tail, we next analyzed the biochemical specificities of the two tyrosine motifs within the cytoplasmic tail of PD-1. For this purpose, we selected SH2 proteins which showed strong PD-1 binding, i.e. Shp1 ($Shp1^{tSH2}$), Shp2 ($Shp2^{tSH2}$) and PI3K(p50α). Consistent with our recent report (Hui, 2017), mutation of either the ITIM or ITSM partially decreased Shp2 binding (Fig. 5C), though mutation of the C-terminal ITSM (Y248) produced a stronger defect. In contrast, mutation of ITSM (Y248) completely abolished Shp1 binding (Fig. 5B), suggesting an exquisite specificity between ITSM and Shp1, but not between ITSM and Shp2. Finally, mutation of either tyrosine motif decreased the binding of the tandem SH2 domains of Shp2 ($Shp2^{tSH2}$) and PI3K (p50α), indicating that both sites contribute to PI3K and SHP2 recruitment (Fig. 5C, Fig. 5D, Fig. 6).

DISCUSSION

BTLA, a T cell co-inhibitory receptor, is a negative regulator of T cell activation. It is commonly believed that BTLA attenuates T lymphocyte activation through recruitment of tyrosine phosphatases. With structural similarity to PD-1, BTLA should, at least partially, resemble PD-1 functionally. Despite the important roles of HVEM/BTLA in regulating the T cell response and tumor immunity, very little is known of the intracellular pathways of BTLA. Using co-immunoprecipitation (co-IP), early studies have found that the phosphatases Shp1, Shp2, SHIP-1, and the adaptor protein Grb2 and PI3K associate with the BTLA cytoplasmic domain upon tyrosine phosphorylation (Watanabe, 2003; Gavrieli 2003; Gavrieli, 2006). However, it is not known how these proteins work together to impact the T cell activity. In addition, the previous co-IP assays did not address whether the protein-protein interactions are direct or indirect.

In this thesis, I employed a well-defined membrane reconstitution system (Hui, 2014) to quantitatively dissect important proteins in the BTLA interactome (Fig. 3). I found that tyrosine phosphorylated BTLA directly recruits Shp1 and Shp2 (Fig. 3A). The abilities of BTLA to recruit these phosphatases are comparable to that of PD-1, with interesting differences in specificity. While PD-1 strongly prefers Shp2 over Shp1, BTLA exhibits similar affinities for with Shp1 and Shp2. It is possible that the ability of BTLA to bind Shp1 might allow BTLA to dephosphorylate a non-overlapping set of proteins from the PD-1/Shp2 complex. Further studies are needed to test this model.

The most striking difference between BTLA and PD-1 is that BTLA also directly recruits the tyrosine kinase ZAP70 (Fig. 3A), whereas PD-1 does not (Fig. 3B, Fig. 3C). ZAP70 is best known to be a central kinase in the TCR pathway. The finding that BTLA

recruits ZAP70 here might indicate some intriguing crosstalk between the TCR and BTLA axis. It is also possible that ZAP70 would allow BTLA to play a positive role in T cell signaling under some scenarios. Further studies are needed to address the physiological relevance and consequence of this interaction.

In addition to protein kinase ZAP70, I also confirm the previous immunoprecipitation report that BTLA associates with PI3K (Gavrieli 2006). Although PD-1 also appeared to recruit PI3K (Fig. 3B), the ability of BTLA to bind PI3K is considerably stronger that PD-1 (Fig. 3C). The functional consequence of this interaction is unknown.

In contrast to previous work by co-IP (Gavrieli, 2006), we did not detect any interaction between BTLA and Grb2 using our direct binding assay. One possibility is that Grb2/BTLA binding might be indirect and require other adaptor proteins. Another possibility is that Grb2/BTLA interaction might be of low affinity, and much higher concentrations of Grb2 is required than available in our system. Because we were using the same concentration of SH2 proteins, we can conclude that if Grb2 binds to BTLA directly, the affinity is much lower than the other SH2 proteins, Shp1, Shp2, PI3K and ZAP70.

In addition to screening for BTLA interactors, we also performed a pairwise comparison between BTLA and PD-1 in the SH2 recruitment assay. We uncovered three major differences between BTLA and PD-1 specificities. Firstly, PD-1 prefers to recruit Shp2 over Shp1, whereas BTLA shows equivalent binding capability to Shp1 and Shp2, according to the time-resolved FRET results. Secondly, recruitment of PI3K to the BTLA

cytoplasmic domain is greater than to PD-1, although both BTLA and PD-1 appear to associate with PI3K. Lastly, BTLA, but not PD-1, binds to ZAP70 in a direct manner.

Different SH2 specificities of BTLA and PD-1 might underlie their non-overlapping roles in regulating the T cell-mediated immunity. Despite the differences, we also show that Shp2 and perhaps PI3K are shared between BTLA and PD-1. These shared effectors might allow BTLA to at least partially compensate for the PD-1 function under physiological context. Notably, it has been reported that compensatory upregulation of BTLA contributes to the resistance of PD-1 blockade therapy in some cancer patients (Zhao, 2016).

Finally, using site-directed mutagenesis in conjunction with the reconstituted membrane FRET assay, we dissected the biochemical specificity of each tyrosine motif in BTLA and in PD-1. The mutation studies indicate that each of the four tyrosine residues within the BTLA cytoplasmic domain display some level of specificities for certain SH2 proteins (Fig. 4). Our biochemical analysis suggests that the third tyrosine (Y257) plays the most important role in recruiting Shp1, Shp2 and ZAP70. The physiological significance of this site needs to be further addressed in T cells and in mouse models. Although single mutations of BTLA cytoplasmic tyrosine analysis cannot sufficiently examine exact binding sites for SH2 proteins, the results reveal the essential tyrosine motifs for SH2 protein recruitment. We predict that the reconstitution system presented in this thesis, combined with classical cell biology and immunological approaches, will be powerful in providing an in-depth molecular understanding of BTLA and other immune checkpoints.

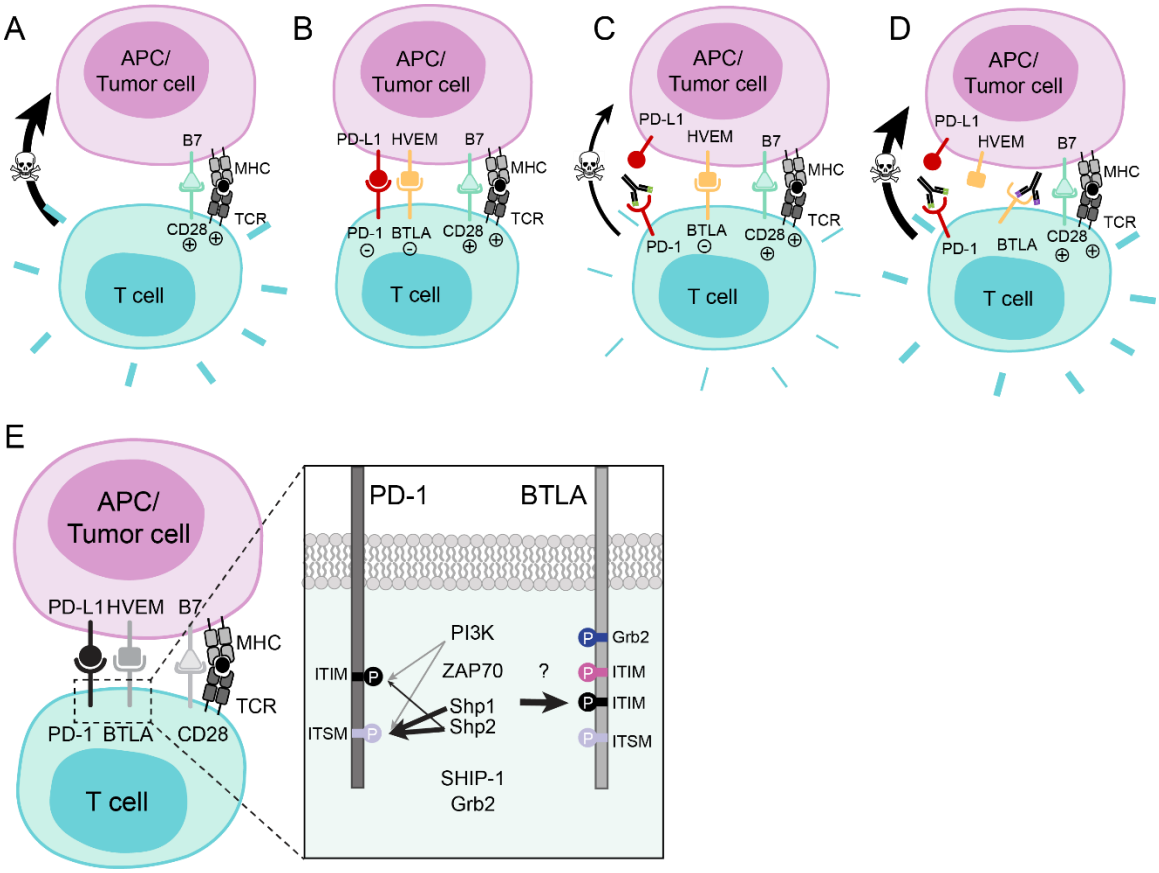

Figure 1. Schematic diagram of T cell activation and inhibition.
(A) T cell signaling paradigm. The thickness of arrows indicates the strength of the interaction. Activation of T cells requires interactions between pMHC and TCR, as well as association of co-stimulatory receptors and their ligands, such as CD28 and B7. Positive signals generated from the TCR and co-stimulatory receptors trigger T cell activation, allowing T cell-mediated infected cell or tumor cell destruction.
(B) In contrast to co-stimulatory receptors, co-inhibitory receptors such as PD-1 and BTLA transduce negative signals to suppress T cell activation.
(C) Monoclonal antibodies that block the interaction between PD-1 and its ligand remove the PD-1-mediated inhibition, so that T cells can be reactivated to destroy tumor cells, at least under some physiological contexts. In many patients, however, blockade of PD-1 is not sufficient to reactivate T cells, potentially due to an inhibitory signal from BTLA or other immune checkpoints (not shown).
(D) Antibody-mediated blockade of both PD-1 and BTLA has been shown to further boost the T cell activity, leading to synergistic rejection of tumors in mouse models.
(E) Previous studies on T cell signaling pathways. Several SH2 domain-containing proteins, including Shp1, Shp2, SHIP1, Grb2 and PI3K (p50α) have been implicated in the BTLA or PD-1 pathway, but the binding specificities are not clear, as indicated by the question mark.

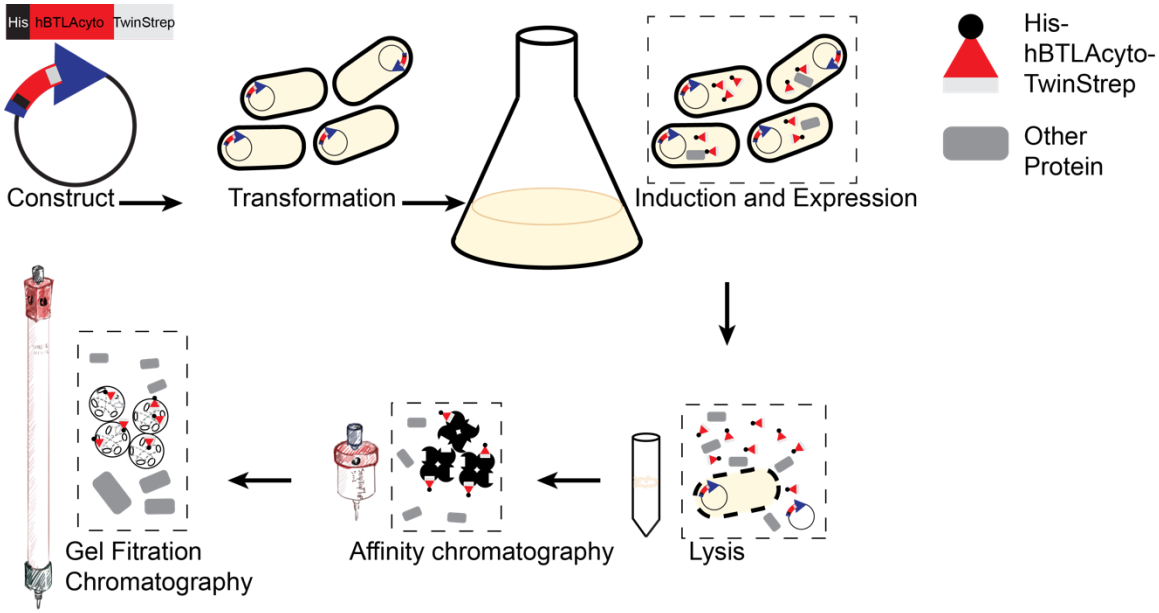

Figure 2. Workflow of BTLA purification.
pET28A plasmid encoding His-hBTLAcyto-TwinStrep was transformed into BL21(DE3) *E. coli*. A single colony was inoculated into LB culture. Protein expression was then induced as described in the Methods. His-hBTLAcyto-TwinStrep was then purified from bacteria cell lysate by using Strep affinity chromatography and gel filtration chromatography. Detailed protocol is described in Material and Method section.

Figure 3. Comparison of BTLA and PD-1 Binding specificities.
(A) (Left) A schematic diagram illustrating a kinetic FRET assay to measure the BTLA binding activities of SH2 proteins. SH2 proteins fused with SNAP tag were labeled with a FRET donor (green star). The liposome membrane was labeled with an FRET acceptor (red star) and reconstituted with both the BTLA cytoplasmic domain and the kinase Lck. Addition of ATP triggered Lck-mediated phosphorylation of tyrosines on the membrane-bound receptor domains. Recruitment of the SH2 protein to the phosphorylated receptor domain decreased the distance between the donors and acceptors, leading to FRET. (Right) Representative time course of the donor fluorescence before and after the addition of ATP. FRET signal was measured as donor quenching.
(B) (Left) A schematic diagram illustrating a kinetic FRET assay to measure the PD-1 binding activities of SH2 proteins. Experiments were conducted in the same manner as in A except for replacing BTLA with an identical concentration of PD-1. (Right) Representative time course of the recruitment of the indicated SH2 proteins to liposome-bound PD-1, as reflected by the quenching of the donor fluorescence.
(C) Pairwise comparisons of BTLA and PD-1 binding activities for each SH2 protein.

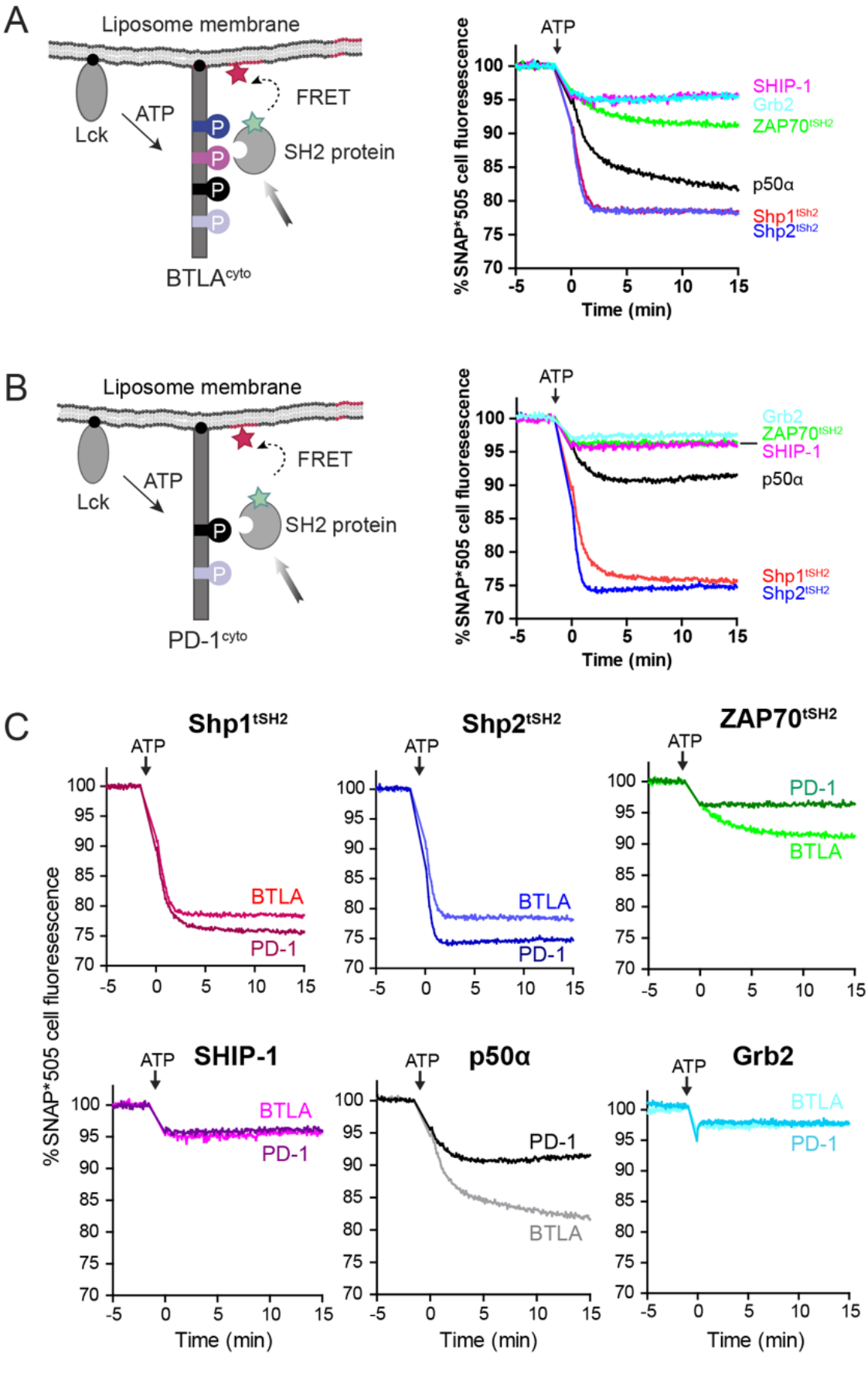
A
Liposome membrane
FRET
ATP
Lck
SH2 protein
BTLA^cyto
ATP
% SNAP*505 cell fluoresescence
SHIP-1
Grb2
ZAP70^tSH2
p50α
Shp1^tSh2
Shp2^tSh2
Time (min)
B
Liposome membrane
FRET
ATP
Lck
SH2 protein
PD-1^cyto
ATP
% SNAP*505 cell fluoresescence
Grb2
ZAP70^tSH2
SHIP-1
p50α
Shp1^tSH2
Shp2^tSH2
Time (min)
C
Shp1^tSH2
Shp2^tSH2
ZAP70^tSH2
SHIP-1
p50α
Grb2
ATP
BTLA
PD-1
% SNAP*505 cell fluoresescence
Time (min)

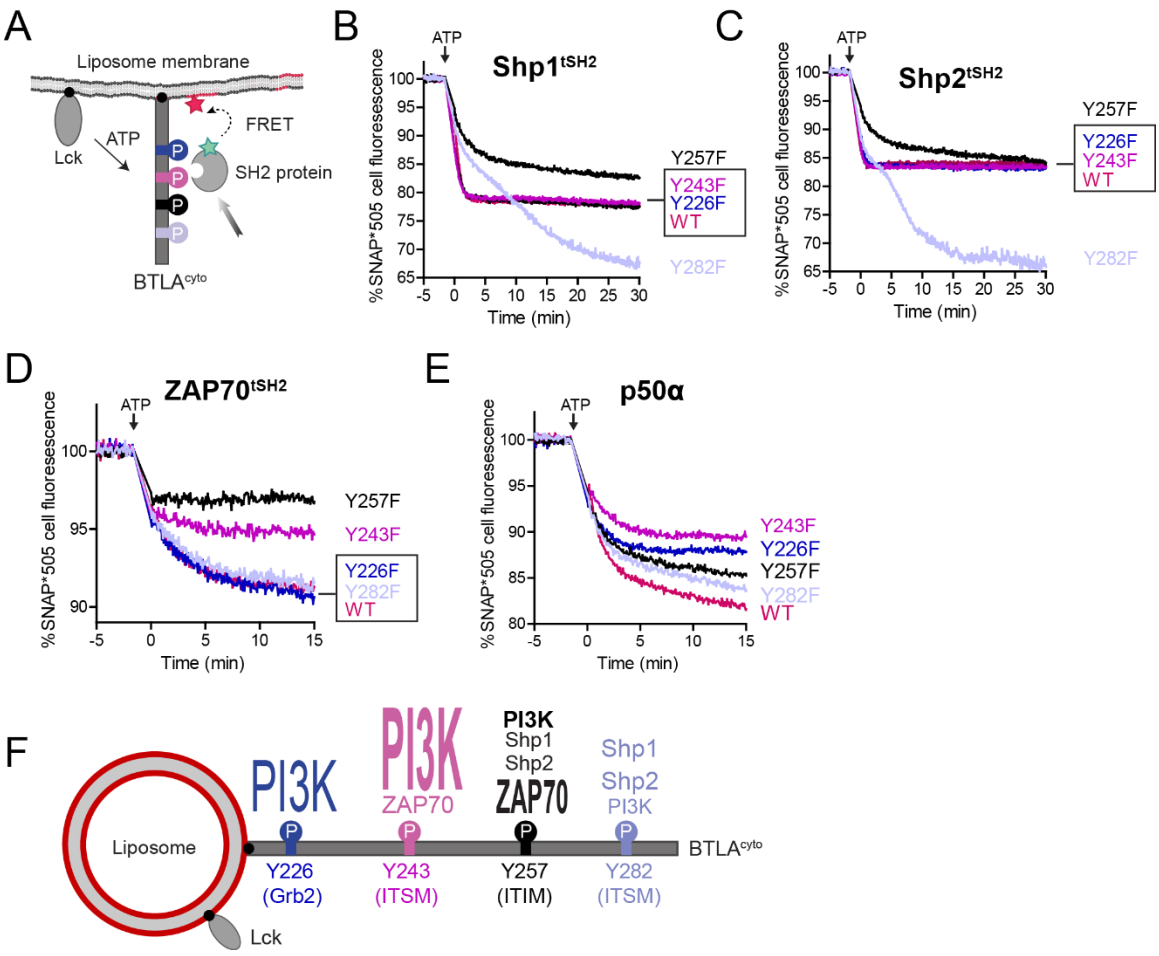

Figure 4. Point mutants of BTLA reveal the binding sites of Shp1, Shp2, ZAP70, and PI3K.

(A) A schematic diagram illustrating a kinetic FRET assay in reconstituted liposome system as shown in Figure 1, with the four tyrosines in the BTLA cytoplasmic tail shown in different colors.

(B) Side by side comparison of the Shp1 binding activities of BTLA WT and the indicated tyrosine mutants. Shown are representative time courses of the donor fluorescence.

(C)-(E) Side by side comparisons of BTLA WT and tyrosine mutants in their abilities to bind $Shp2^{tSH2}$, $ZAP70^{tSH2}$, and p50α . Experiments were conducted in the same manner as in B except replacing $Shp1^{tSH2}$ with the same concentration of $Shp2^{tSH2}$, $ZAP70^{tSH2}$ or p50α.

(F) A working model showing the binding sites within the BTLA cytoplasmic domain for each SH2 protein tested. The sizes of the font indicate the relative strength of the interaction observed in (B)-(E).

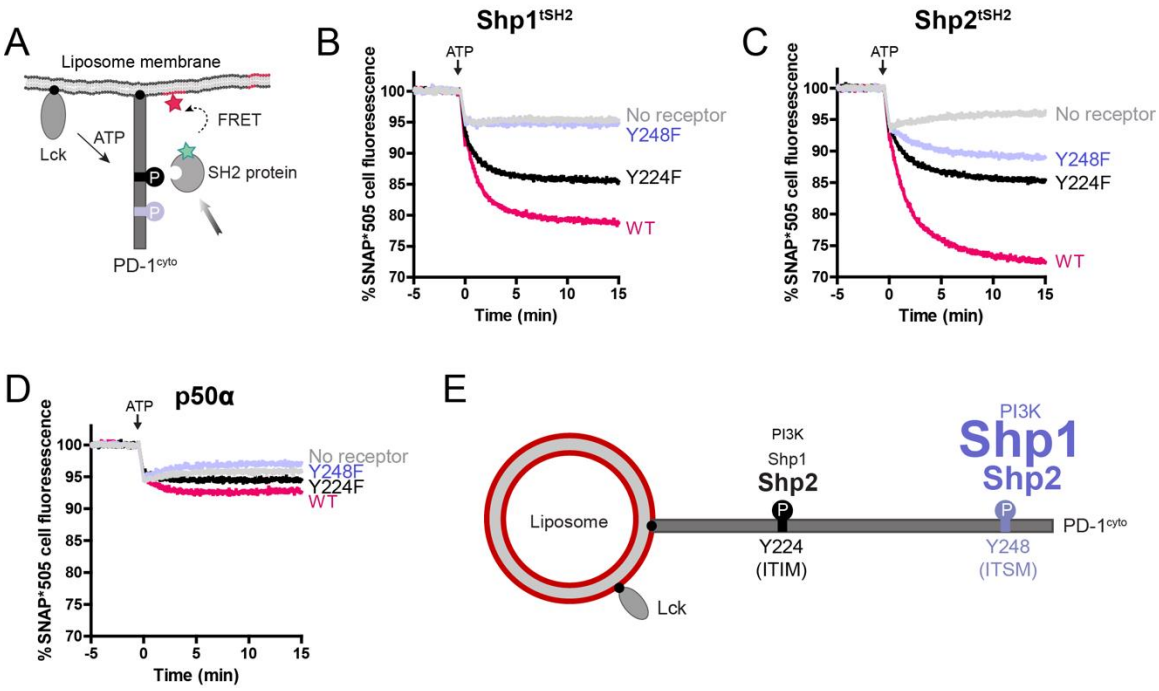

Figure 5. Point mutants of PD-1 reveal the binding sites of Shp1, Shp2, and PI3K.
(A) A schematic diagram illustrating a kinetic FRET assay in the reconstituted liposome system, with the two tyrosines in the PD-1 cytoplasmic tail shown in different colors.
(B) Side by side comparison of the Shp1^{tSH2} binding activities of PD-1 WT and the indicated tyrosine mutants. Shown are representative time course of the donor fluorescence.
(C) Side by side comparison of the Shp2^{tSH2} binding activities of PD-1 WT and the indicated tyrosine mutants. Shown are representative time course of the donor fluorescence.
(D) Side by side comparison of the p50α binding activities of PD-1 WT and the indicated tyrosine mutants. Shown are representative time course of the donor fluorescence.
(E) A working model depicting binding sites within the PD-1 cytoplasmic domain for each SH2 protein tested. The font sizes indicate the relative strength of the association observed in (B)-(D).

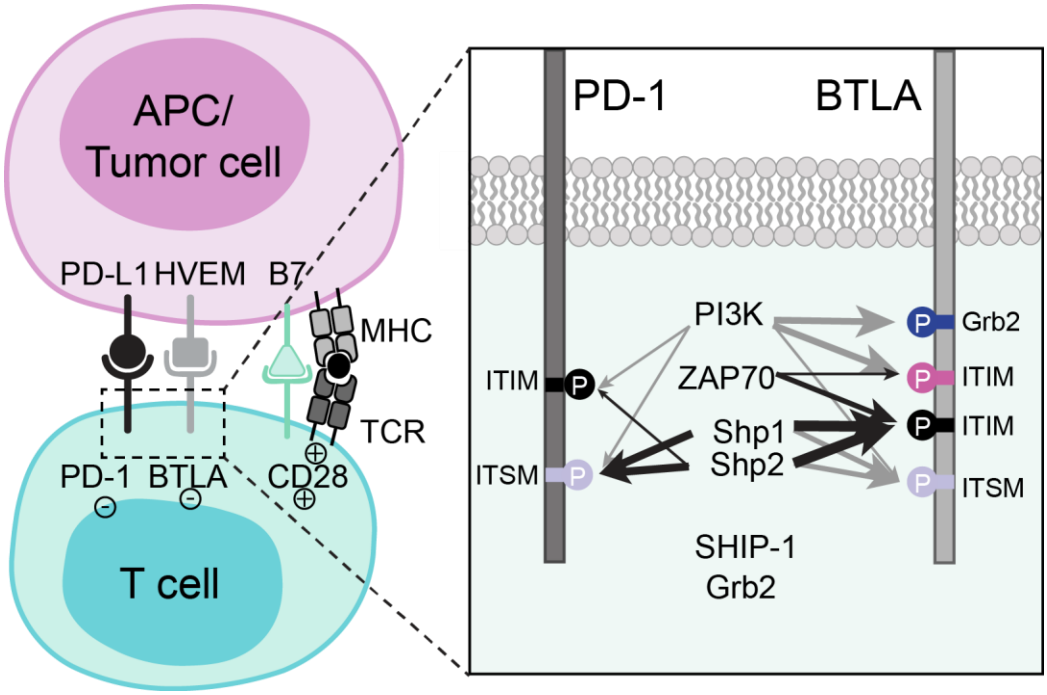

Figure 6. Model summarizing the findings in the thesis.
An overview diagram of how PD-1 and BTLA function in T cell co-signaling network. Ligand binding to the extracellular domain of PD-1 and BTLA triggers tyrosine phosphorylation of their cytoplasmic tails, which leads to recruitment of certain SH2 containing proteins. Shown on the right is a zoomed in view of the intracellular tail of both PD-1 and BTLA, and SH2 proteins that interact with them. The thickness of the arrows indicates the strength of the binding interactions.

REFERENCE

1. Chen, L., and Flies, D. BD. Molecular mechanisms of T cell co-stimulation and co-inhibition. *Nat. Rev. Immunol*. **13**, 227-242 (2013).

2. del Rio, M. L., Lucas, C. L., Buhler, L., Rayat, G., and Rodriguez-Barbosa, J. I. HVEM/LIGHT/BTLA/CD160 cosignaling pathways as targets for immune regulation. *J. Leukoc. Biol.* **87(2)**, 223-235 (2010).

3. Deppong, C., Juehne, T. I., Hurchla, M., Friend, L. D., Shah, D. D., Rose, C. M., Bricker, T. L., Shornick, L. P., Crouch, E. C., Murphy, T. L., Holtzman M. J., Murphy, K. M., and Green, J. M. Cutting edge: B and T lymphocyte attenuator and programmed death receptor-1 inhibitory receptors are required for termination of acute allergic airway inflammation. *J. Immunol.* **176**, 3909–3913 (2006).

4. Gavrieli, M., Watanabe, N., Loftin, S. K., Murphy, T. L., and Murphy, K. M. Characterization of phosphotyrosine binding motifs in the cytoplasmic domain of B and T lymphocyte attenuator required for association with protein tyrosine phosphatases SHP-1 and SHP-2. *Biochem. Biophys. Res. Commun.* **312**, 1236-1243. (2003).

5. Gavrieli, M. and Murphy, K. M. Association of Grb-2 and PI3K p85 with phosphotyrosile peptides derived from BTLA. *Biochem. Biophys. Res. Commun.* **345**, 1440–1445 (2006).

6. Han, P., Guolarte, O. D., Rufner, K., Wilkinson, B., and Kaye, J. An inhibitory Ig superfamily protein expressed by lymphocytes and APCs is also an early marker of thymocyte positive selection. *J. Immunol.* **172**, 5931–5939 (2014).

7. Hui, E., and Vale, R. D In vitro membrane reconstitution of the T-cell receptor proximal signaling network. *Nat. Struct. Mol. Biol.* **21**, 133–142(2014). doi:10.1038/nsmb.2762pmid:24463463

8. Ishida, Y., Y. Agata, K. Shibahara, and T. Honjo. Induced expression of PD-1, a novel member of the immunoglobulin gene superfamily, upon pro- grammed cell death. *EMBO J.* **11**, 3887 (1992).

9. Latchman, Y., Wood, C. R., Chernova, T., Borde, M., Chernova, I., Iwai, Y., Long, A. J., Brown, J. A., Nunes, R., Greenfield, E.A., Bourque, K., Boussiotis, V. A., Cater, L. L., Carreno, B. M., Malenkovich, N., Nishimura H., Okazaki, T., Honjo, T., Sharpe, A. H., and Freeman, G. J. PD-L2 is a second ligand for PD-I and inhibits T cell activation. *Nat. Immunol*. **2**, 261–268 (2001).

10. Otsuki, N., Kamimura, Y., Hashiguchi, M., and Azuma, M. Expression and function of the B and T lymphocyte attenuator (BTLA/CD272) on human T cells. *Biochem. Biophys. Res. Commun.* **344**, 1121–1127 (2006).

11. Okazaki, T., Iwai, Y., and Honjo, T. New regulatory co-receptors: inducible co-stimulator and PD-1. *Curr. Opin. Immunol.* **14**,779-782 (2002).

12. Paradoll, D. M. The blockade of immune checkpoints in cancer immunotherapy. *Net. Rev. Cancer*. **12(4)**, 252-264 (2012).

13. Parry, R. V., Chemnitz, J. M., Frauwirth, K. A., Lanfranco, A. R., Braunstein, I., Kobayashi, S. V., Linsley, P. S., Thompson, C. B., and Riley, J. L. CTLA-4 and PD-1 Receptors Inhibits T-cell Activation by Distinct Mechanisms. *Mol. Cell. Bio.* **25(21)**, 9543-9553 (2005).

14. Watanabe, N., Gavrieli, M, Sedy, J. R., Yang, J., Fallarino, F., Loftin, S. K., Hurchla, M. A., Zimmerman, N., Sim, J., Zang, X., Murphy, T. L., Russel, J., H., Allison, J. P., and Murphy, K. M. BTLA is a lymphocyte inhibitory receptor with similarities to CTLA-4 and PD-1. *Nat. Immunol*.**4**, 670-679 (2003)

15. Wang, Y., Subdhi, S. K., Anders, R. A., Lo, J., Sun, Y., Blink, S., Wang, Y., Liu, Xu., Mlink, K., Degradi, D., Pfeffer, K., and Fu, Y. X. The role of herpesvirus entry mediator as a negative regulator of T cell-mediated responses. *J. Clin. Invest.* **115**, 711–717 (2005).

16. Wherry, J. E., and Kurachi, M. Molecular and cellular insights into T cell exhaustion. Nat. Rev. Immunol. **15(8)**, 486-499 (2015).

17. Wu, P. G., and Brand, L. Resonance Energy Transfer: Methods and Applications. *Analytical Biochemistry*. **216**, 1-13 (1994).

18. Yokosuka, T., Takamatsu, M., Kobayashi-Imanishi, W., Hashimoto-Tane, A., Azuma, M., and Saito, T. Programmed cell death 1 forms negative costimulatory microcluster that directly inhibit T cell receptor signaling by recruiting phosphatase Shp2. **209(6)**, 1201-1217 (2012).

19. Zhao, Q., Huang, Z. L., He, M., Gao, Z., and Kuang, D. M. BTLA identifies dysfunctional PD-1-expressing CD4(+) T cells in human hepatocellular carcinoma. *Oncoimmunology*. **5(12)**, p. e1254811 (2016).